

## Soft switched DC-DC PWM Converters

Mr.M. Prathap Raju<sup>(1)</sup>, Dr. A. Jaya Lakshmi<sup>(2)</sup>

**Abstract** – This paper presents an upgraded soft switching technique- zero current transition (ZCT), which gives better turn off characteristics for the switching devices than conventional ZVS. An auxiliary circuit is augmented for the converter, which implements Zero Current Transition by incorporating the concept of resonance for all the switching elements. The proposed zero current transition is designed for DC-DC buck, fly back, Boost converters and the same is simulated for a frequency of 10kHz by using MATLAB-Simulink. The main emphasize is on the analysis of switching stress (di/dt) and switching losses of the various converters simulated. Analytical comparison presented with hard and soft switching proves the superiority of the proposed soft switched converters over conventional.

Index Terms – PWM, DC to DC, buck, boost, fly back, Zero Current Transition (ZCT)

### I. INTRODUCTION

PULSE WIDTH Modulated (PWM) dc/dc converters are vastly used in industry because of their high-power capability and fast transient response. To reduce the volume and the weight of these converters, higher switching frequency operation is preferred. In high power frequency requirements, power semiconductor switches are subjected to high switching stresses and switching losses, which limits the operating switching frequency. Generally, a snubber circuit reduces the switching losses and stresses, but increases the total power loss in the converter. In resonant and quasi-resonant converters, the switching losses are reduced; however, the converter control system is usually a frequency control instead of a PWM control. Furthermore, in these converters, high voltage or current stresses are applied to semiconductor devices due to the nature of the resonance. Zero Current Transition (ZCT) and Zero-Voltage Transition (ZVT) techniques incorporate a soft switching function into standard PWM converters [1]–[9]; thus, the switching losses can be reduced. In these converters, an auxiliary circuit is added to the main PWM converter, which functions only at switching instances and recovers the switching losses. For high-power applications, an Insulated Gate Bipolar Transistor (IGBT) is the preferred device. However, the IGBT exhibits tailing current at turnoff, which increases turnoff switching losses. Hence, ZCT techniques provide better results than ZVT techniques. Several ZCT converters have been previously proposed in [1]–[9], but they suffer from one or more of the following drawbacks.

1) In some topologies, the main switch turn-on is not soft and, thus, limits the gain in efficiency [1].

2) The main switch peak current is increased considerably [2]–[4].

3) The switches turn off are not soft [5].

4) There are additional semiconductor devices in the main power path that increase conduction losses [6], [7].

5) The proposed technique cannot be applied to fly back converters [1], [2], [5].

A new family of ZCT converters lacking the aforementioned disadvantages was introduced [9]. In these converters, the main switch and the auxiliary switch are turned on and off under Zero-Current (ZC) condition, so that the switching losses and stresses are significantly reduced. The energy of the proposed auxiliary circuit is absorbed from the input voltage source and is transferred to the output, which boosts the effective output duty cycle. However, in other converters, usually, the auxiliary circuit energy is just a circulating energy [1],[2],[5]–[9]. One of the advantages of the proposed auxiliary circuit is that it can be applied to fly back converters. A ZCT fly-back converter was introduced in [4], which has disadvantages in comparison to the proposed ZCT fly back as discussed in Section V. The idea of the proposed auxiliary circuit is discussed in section II. The ZCT buck converter was analyzed in [1]; however, since it is the base of this converter family, its operation is briefly discussed in Section III. In Section IV, fly back ZCT converter is explained. As the requirement of boost converter is high in industries, detailed performance characteristics are detailed in section IV. The performance parameters derived for different ZCT PWM converters are presented in Section V. Simulation results and comparative analysis for the same is presented in the proceeding sections.

### II. AUXILIARY CIRCUIT DERIVATION

Generally, in non isoated fundamental converters, one way to create ZC condition for switch turn-on is to have a snubber inductor in series with the switch or diode. However, at turnoff, this inductor will cause a voltage spike on the switch. Therefore, a pulse current source is required to provide the output current, and, thus, the switch can be turned off under ZC condition while preventing the voltage spikes. To reduce the number of circuit elements, the pulse current source path and the required snubber inductor to decrease turn-on losses can be combined as shown in Fig. 1 for a buck converter. A pulse voltage source can be applied to the snubber inductor and create the required pulse current source at switch turnoff. Design of resonant inductance and capacitance should be done such that the underdamped nature of the LC circuit at a certain resonant frequency is ensured. Switching frequency of main

and auxiliary switches is to be considered with the reference of the resonant frequency for which the LC components are designed.

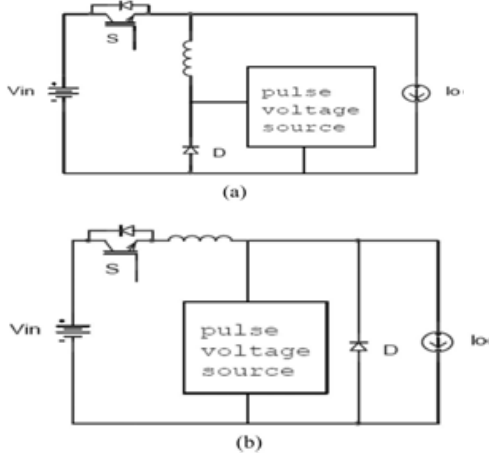


Fig.1 Schematic ZCT buck converter (a) Snubber Inductor in series with a diode and (b) Snubber inductor in series with a switch.

### III. ZCT BUCK CONVERTER DESCRIPTION

The proposed ZCT buck converter is shown in Fig.2. The circuit is composed of the main switch  $S$ , the main diode  $D$ , the auxiliary switch  $S_a$ , the auxiliary diode  $D_a$ , the auxiliary inductors  $L_{a1}$  and  $L_{a2}$ , and the auxiliary capacitor  $C_a$ .  $L_{a1}$  is the snubber inductor, and the pulse voltage source is basically represented by  $C_a$  and  $S_a$ .  $L_{a2}$  and  $D_a$  are used to recharge the capacitor at every cycle. The converter has seven distinct operating intervals during one switching cycle. Before the first interval, it is assumed that the auxiliary capacitor is charged to  $2V_{in}$ , and the main switch is conducting. Key theoretical waveforms of the converter are shown in Fig. 3.

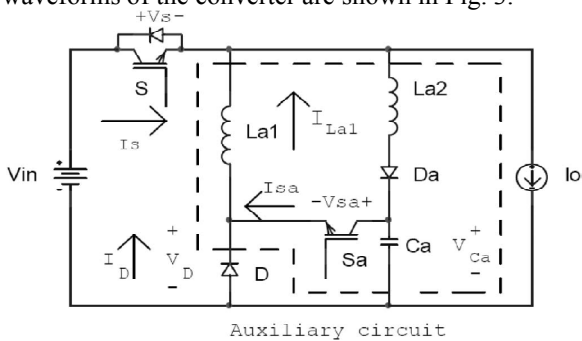


Fig.2 Proposed ZCT buck converter.

**Interval 1 [t<sub>0</sub>–t<sub>1</sub>]:** This interval begins with turning the auxiliary switch on. This starts a resonance between the auxiliary capacitor  $C_a$  and the auxiliary inductor  $L_{a1}$ . During this resonance, the  $L_{a1}$  current increases until it reaches the output current  $I_o$  and reduces the switch current to zero.

**Interval 2 [t<sub>1</sub>–t<sub>2</sub>]:** In this interval, the main switch body diode starts to conduct, and the resonance between the auxiliary inductor  $L_{a1}$  and the auxiliary capacitor  $C_a$  will continue.

Thus, the main switch can be turned off under the ZC condition before the  $L_{a1}$  current is reduced back to the output current  $I_o$ .

**Interval 3 [t<sub>2</sub>–t<sub>3</sub>]:** In this interval, the  $L_{a1}$  current is equal to  $I_o$ , and the auxiliary capacitor linearly discharges until its voltage becomes zero at the end of this interval.

**Interval 4 [t<sub>3</sub>–t<sub>4</sub>]:** This interval starts when the main diode begins to conduct under the zero-voltage condition, and the auxiliary switch can be turned off under the ZC condition. In this interval, the main diode current and the  $L_{a1}$  current are equal to  $I_o$ . This interval ends when the main switch is turned on.

**Interval 5 [t<sub>4</sub>–t<sub>5</sub>]:** When the main switch is turned on, the  $L_{a1}$  current begins to linearly decrease, and the  $L_{a2}$  current starts to increase in a resonance fashion with  $C_a$ . Therefore, the main switch turns on under the ZC condition.

**Interval 6 [t<sub>5</sub>–t<sub>6</sub>]:** This interval starts when the current of  $L_{a1}$ , which flows through the main diode, reaches zero, and the main diode turns off under the ZC condition. At the end of this interval, the resonance between  $L_{a2}$  and  $C_a$  ends when  $C_a$  is charged to  $2V_{in}$ , and  $D_a$  prevents the current from going negative.

**Interval 7 [t<sub>6</sub>–t<sub>0</sub> + T]:** The output current  $I_o$  runs through the main switch, and the circuit behaves like a regular PWM buck converter.

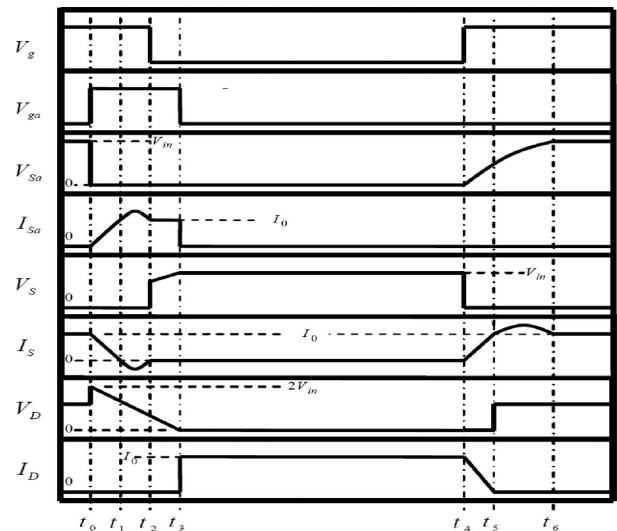
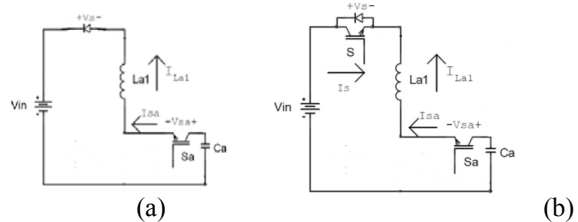


Fig.3 Key theoretical waveforms of the ZCT buck converter.



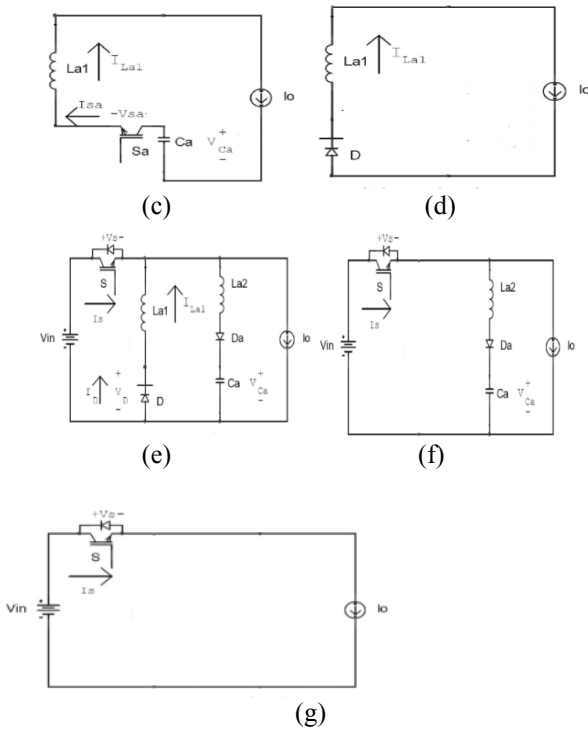


Fig.4 Equivalent circuit for each operating interval of the proposed ZCT buck converter. (a) ( $t_0 - t_1$ ). (b) ( $t_1 - t_2$ ). (c) ( $t_2 - t_3$ ). (d) ( $t_3 - t_4$ ). (e) ( $t_4 - t_5$ ). (f) ( $t_5 - t_6$ ). (g) ( $t_6 - t_0+T$ )

**IV ZCT FLYBACK CONVERTER DESCRIPTION**

An equivalent circuit for each operating interval of the improved ZCT Fly-back converter (Fig. 5) is shown in Fig. 7, and the main theoretical waveforms are illustrated in Fig. 6,  $I_p$  is the transformer magnetizing current in the primary side, and  $LL$  is the transformer leakage inductance. The transformer magnetizing inductance is assumed to be large enough, so that the transformer total ampere-turns are considered constant in a switching cycle. Before the first interval, it is assumed that the  $Ca$  voltage is  $V/1$ , and the main switch is conducting. The converter operating modes are as follows.

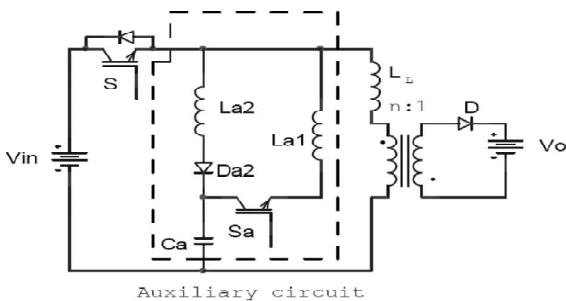


Fig.5 proposed Improved ZCT flyback converter

**Interval 1 [ $t_0-t_1$ ]:** The auxiliary switch is turned on, and a resonance between  $Ca$  and  $La1$  begins. When the  $La1$  current

reaches  $I_p$ , The main switch is turned off under the ZC condition.

$$\omega_1 = \frac{1}{\sqrt{L_{a1} \cdot C_a}}$$

**Interval 2 [ $t_1-t_2$ ]:** The resonance between  $La1$  and  $Ca$  will continue, and the resonance current increases beyond  $I_p$  causing the body diode of the main switch to conduct. When the  $La1$  current returns back to  $I_p$ , the body diode of the main switch turns off.

**Interval 3 [ $t_2-t_3$ ]:** The  $La1$  current is constant and equal to  $I_p$ . Therefore,  $Ca$  is linearly discharged until its voltage reaches  $-nV_0$ , and the rectifying diode  $D$  is forward biased. During this interval, the energy stored in  $Ca$  is transferred to the output, which is equivalent to boosting the effective duty cycle.

**Interval 4 [ $t_3-t_4$ ]:** Since  $D$  is conducting and the voltage across the primary side of the transformer is constant, a resonance starts between  $La1$ ,  $LL$ , and  $Ca$ . During this resonance,  $La1$  and  $LL$  currents decrease, and the  $D$  current increases to  $I_p$ .

$$\omega_2 = \frac{1}{\sqrt{(L_{a1} + L_1) \cdot C_a}}$$

**Interval 5 [ $t_4-t_5$ ]:** During a resonance between  $La2$ ,  $LL$  and  $Ca$ ,  $Ca$  is charged. Where

$$\omega_3 = \frac{1}{\sqrt{(L_{a2} + L_1) \cdot C_a}}$$

**Interval 6 [ $t_5-t_6$ ]:** Diode  $D$  is conducting, and the converter behaves like a regular flyback converter

**Interval 7 [ $t_6-t_7$ ]:** The main switch is turned on under the ZC condition due to the transformer leakage inductance. At the same time, a slow resonance starts between  $La2$  and  $Ca$ , in which its effect can be ignored until the next interval. At the end of this interval, the main switch current is  $I_p$ , and diode  $D$  turns off.

**Interval 8 [ $t_7-t_8$ ]:**  $Ca$  is charged in a resonance with  $La2$ . Where

$$\omega_4 = \frac{1}{\sqrt{L_{a2} \cdot C_a}}$$

**Interval 9 [ $t_8-t_0 + T$ ]:** The main switch is conducting, and the converter behaves like a regular flyback converter.

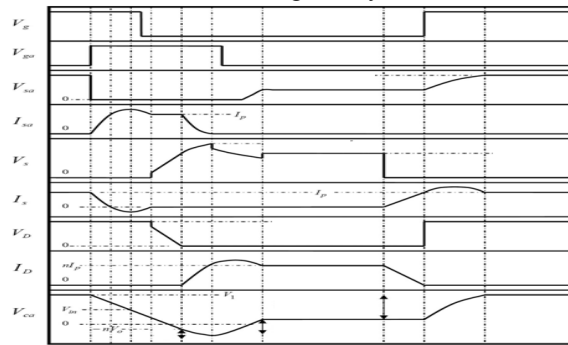


Fig.6 Main theoretical waveforms of the ZCT flyback converter

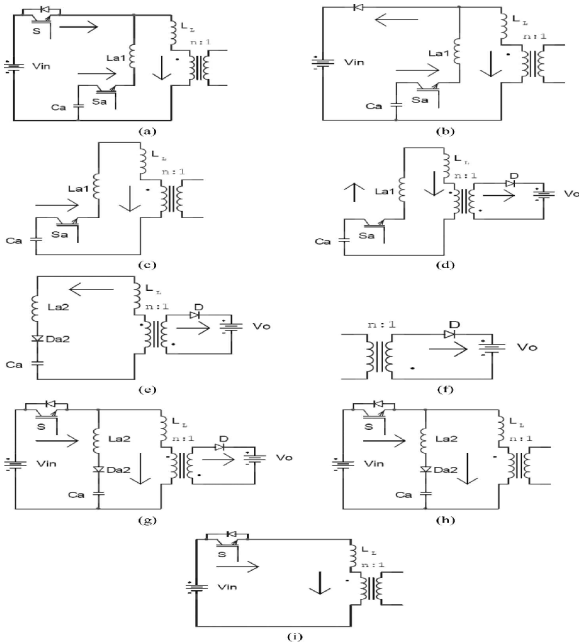


Fig.7 Equivalent circuit for each operating interval of the improved ZCT flyback converter. (a) (t0 - t1). (b) (t1 - t2). (c) (t2 - t3). (d) (t3 - t4). (e) (t4 - t5). (f) (t5 - t6). (g) (t6 - t7). (h) (t7 - t8). (i) (t8 - t1 + T).

**V. DESIGN AND PERFORMANCE PARAMETERS:**

**FOR ZCT BUCK CONVERTER:**

**DESIGN PARAMETERS:**

Assumed that  $C_a = 1 \mu F$

Resonant Frequency  $f_r = 10 \text{ kHz}$

$$\omega_1 = \frac{1}{\sqrt{L_{a1} \cdot C_a}} ; L_{a1} = 25.33 \text{ mH}$$

$$\omega_2 = \frac{1}{\sqrt{L_{a2} \cdot C_a}} ; L_{a2} = 25.33 \text{ mH}$$

**PERFORMANCE PARAMETERS**

Input voltage

$V_i = 250 \text{ v}$

Duty cycle

$K = 0.25, 0.5, 0.75, 1$

Output voltage

$$V_o = \left( \frac{T_{on}}{T} \right) \cdot V_i$$

$V_i$	$K$	$V_o$
250	0.25	62.5
250	0.5	125
250	0.75	187.5
250	1	250

**FOR ZCT FLYBACK CONVERTER**

**DESIGN PARAMETERS:**

Assumed that  $C_a = 1 \mu F$

Resonant Frequency  $f_r = 10 \text{ kHz}$

Leakage inductance  $L_L = 2 \mu H$

$$\omega_1 = \frac{1}{\sqrt{L_{a1} \cdot C_a}}$$

$$L_{a1} = 25.33 \text{ mH}$$

$$\omega_4 = \frac{1}{\sqrt{L_{a2} \cdot C_a}}$$

**PERFORMANCE PARAMETERS**

Input voltage

$V_i = 250 \text{ v}$

Duty cycle

$K = 0.25, 0.5, 0.75, 1.$

Transformer turns

Ratio:  $N_2/N_1 = 1$

Output voltage =

$V_i$	$K$	$V_o$
250	0.25	83.33
250	0.5	250
250	0.75	750

$$V_o = \left( \frac{\left( \frac{N_2}{N_1} \right) \cdot V_s \cdot K}{1 - K} \right)$$

**FOR ZCT BOOST CONVERTER:**

The performance of the ZCT boost converter is also similar to the remaining converters. Design and performance parameters are detailed here below.

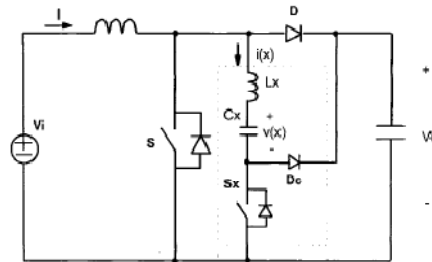


Fig.8 ZCT Boost converter

**DESIGN PARAMETERS:**

Assume that  $C_x = 1 \mu F$

Frequency  $f_r = 10 \text{ kHz}$

$$\omega_1 = \frac{1}{\sqrt{L_{a1} \cdot C_a}}$$

$$L_x = 2.533 \text{ mH}$$

**PERFORMANCE PARAMETERS**

Input voltage

$$V_i = 250 \text{ v}$$

Duty cycle

$$K=0.25, 0.5, 0.75, 1$$

$$V_o = \left( \frac{1}{1 - K} \right) \cdot V_i$$

$V_i$	$K$	$V_o$
250	0.25	333.33
250	0.5	500
250	0.75	1000

**VI. SIMULATION RESULTS**

With reference to the design and performance parameters, the proposed ZCT converters and conventional converters for a frequency are simulated. Simulated models along with results are detailed here below.

**a. SIMULINK MODEL FOR HARD SWITCHED BUCK CONVERTER AT  $F_s=10 \text{ kHz}$**

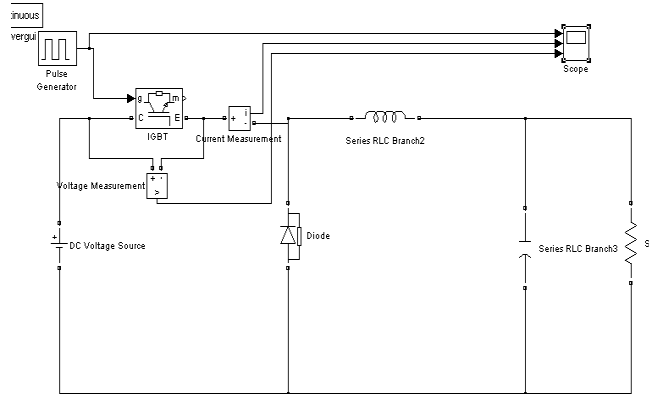


Fig.9 Simulink model for hard switched buck converter

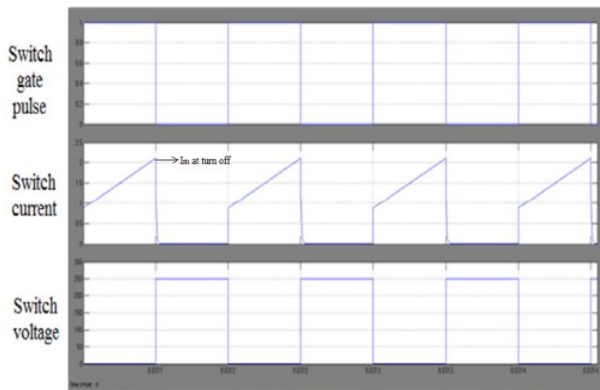


Fig.10 waveforms for hard switched buck converter

**b. SIMULATION MODEL FOR PROPOSED ZERO CURRENT TRANSITION BUCK CONVERTER AT  $F_s = 10 \text{ kHz}$**

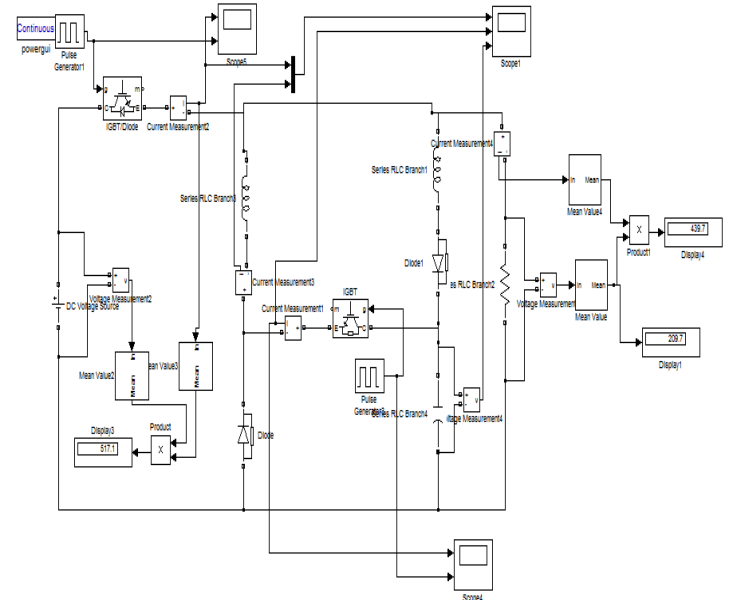


Fig.11 Simulink model for proposed ZCT Buck converter

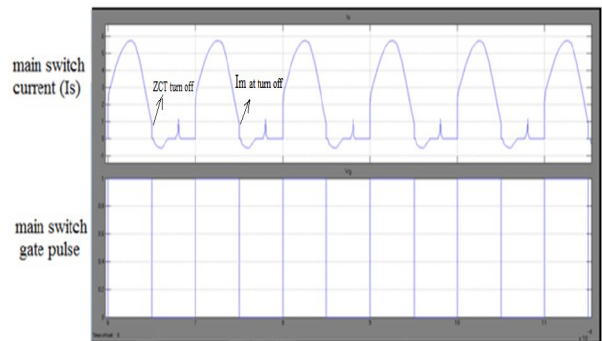


Fig.12 Main switch gate pulse and current waveforms (soft switched buck converter)

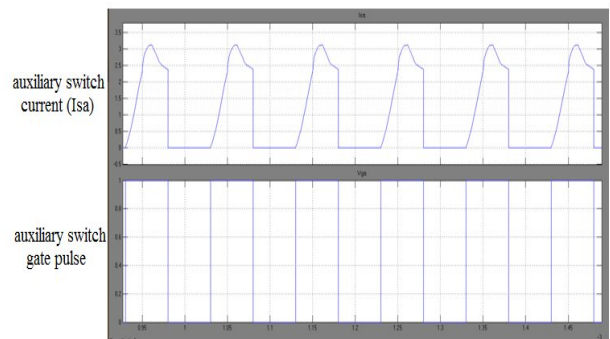


Fig.13 Auxiliary switch gate pulse and current waveforms

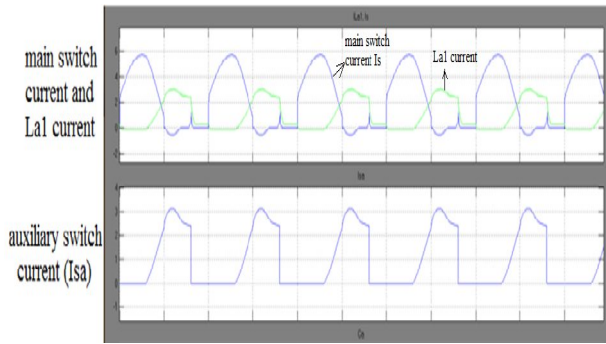


Fig.14 Waveforms of ZCT buck converter

**c. SIMULINK MODEL FOR HARD SWITCHED FLYBACK CONVERTER AT  $F_s=10$  kHz**

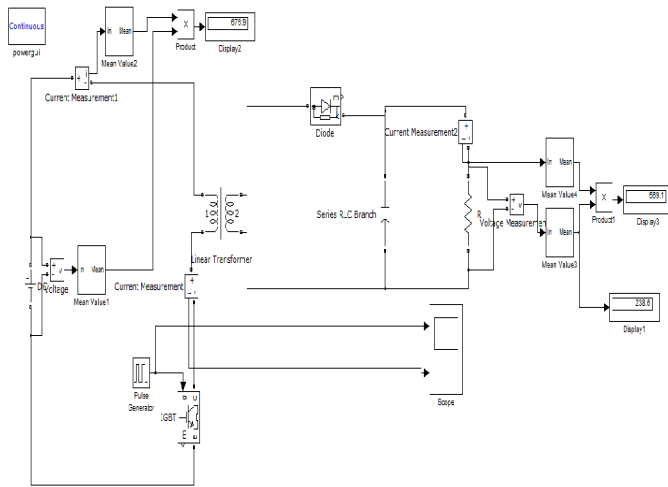


Fig.15 simulink model for hard switched flyback converter

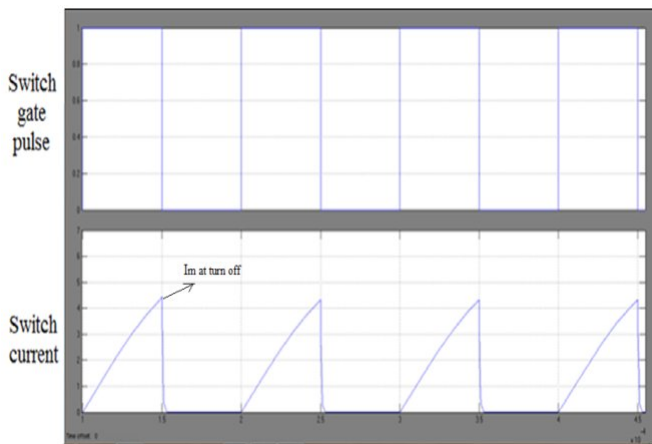


Fig.16 waveforms of hard switched flyback converter

**d. SIMULINK MODEL FOR ZCT FLYBACK CONVERTER**

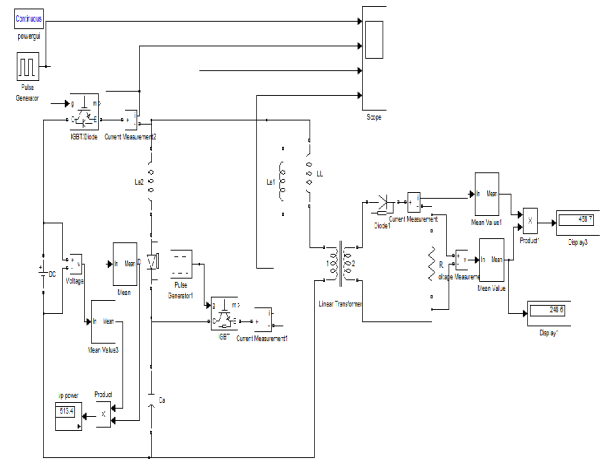


Fig.17 Simulink model for ZCT flyback converter

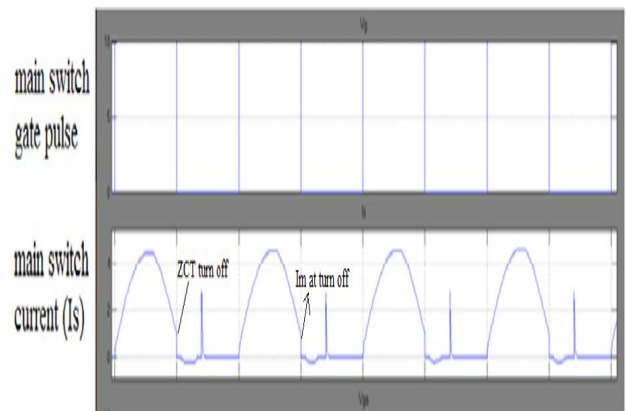


Fig.18 Waveforms of ZCT flyback converter

**e. SIMULINK MODEL FOR HARD SWITCHED BOOST CONVERTER**

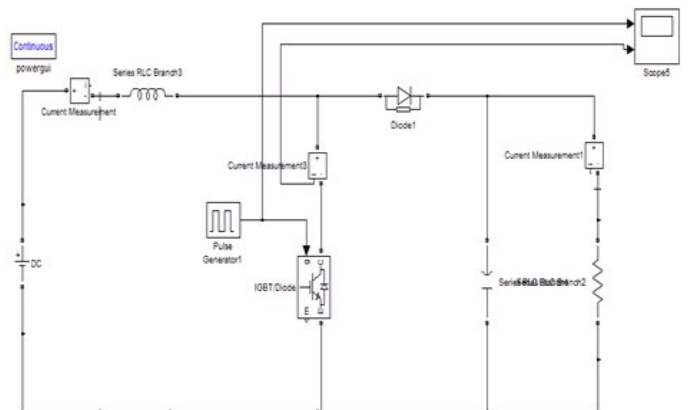


Fig.19 Simulink model for hard switched boost converter



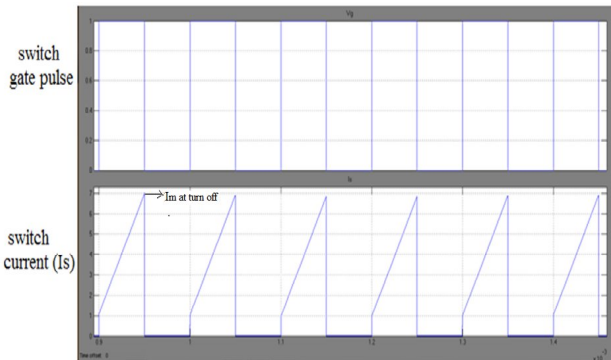


Fig.20 Waveforms of hard switched boost converter

**f. SIMULINK MODEL FOR ZCT BOOST CONVERTER**

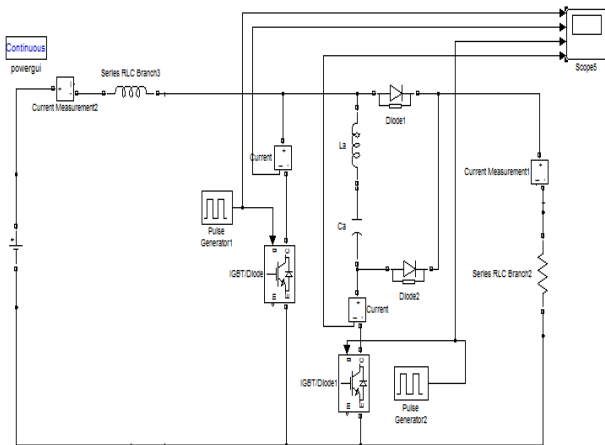


Fig.21 Simulink model for ZCT boost converter

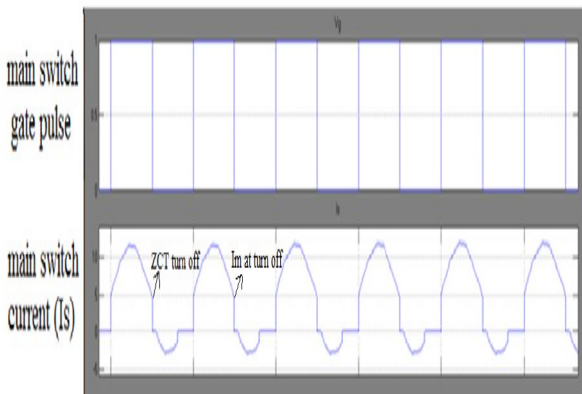


Fig.22 Waveforms of ZCT boost converter

**VII. ANALYSIS OF SWITCHING LOSS AND STRESS**

The proposed topologies with Zero current Transition and conventional hard switched are analyzed based on the simulated results obtained. Calculation of the very important factors switching (power) loss and stress are done and are detailed here below .

**Switching loss during the switching transition:**

$$P_{loss} = \frac{1}{2} V_i \cdot I_m f_s (t_f)$$

**Switching stress:**

di/dt rating across the switch when the switch is turned off:

$$\frac{di}{dt} = \frac{\text{Transition in current during fall time}}{\text{Fall time}}$$

As per the performance parameters figured in the earlier section. Detailed analysis is given below.

**FOR HARD SWITCHED BUCK CONVERTER**

$V_i = 250 \text{ v}$ ,  
 $I_m = 2.1 \text{ A}$  (as per the figure 10)  
 $F_s = 10 \text{ kHz}$   
 and fall time of switching transition(assumed)  $T_f = 3 \mu\text{s}$   
 Switching powerloss :  $P_{loss} = 7.87 \text{ watts}$   
 Switching stress:  $\frac{di}{dt} = 0.7 \text{ A} / \mu\text{sec}$

**FOR SOFT SWITCHED BUCK CONVERTER**

The current through the switch is modulated such that  
 $I_m = 0.9 \text{ A}$  (as shown in figure 12), other parameters remain same.  
 Switching Power loss:  $P_{loss} = 3.37 \text{ watts}$   
 Switching stress:  $\frac{di}{dt} = 0.3 \text{ A} / \mu\text{sec}$

**FOR HARD SWITCHED FLYBACK CONVERTER**

$I_m = 4.5 \text{ A}$  (as shown in figure 16 ), other parameters remain same.  
 Switching Power loss:  $P_{loss} = 16.87 \text{ watts}$   
 Switching stress:  $\frac{di}{dt} = 0.3 \text{ A} / \mu\text{sec}$

**FOR SOFT SWITCHED FLYBACK CONVERTER**

$I_m = 1 \text{ A}$  (as shown in figure 18), other parameters remain same.  
 Switching power loss:  $P_{loss} = 3.75 \text{ watts}$   
 Switching stress:  $\frac{di}{dt} = 0.3 \text{ A} / \mu\text{sec}$

**FOR HARD SWITCHED BOOST CONVERTER**

$I_m = 7A$  (as shown in figure 20), other parameters remain same.

Switching power loss:

$$P_{\text{loss}} = 26.25 \text{ watts}$$

$$\frac{di}{dt} = 2.33 \text{ A} / \mu \text{ sec}$$

**FOR SOFT SWITCHED BOOST CONVERTER**

$I_m = 2A$  (as shown in figure 22 ), other parameters remain same.

Switching power loss:  $P_{\text{loss}} = 7.50 \text{ watts}$

$$\frac{di}{dt} = 0.66 \text{ A} / \mu \text{ sec}$$

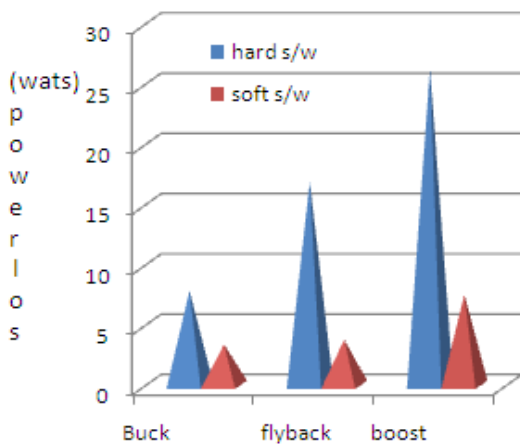
**Switching loss analysis:**

Fig.23 graphical view of power loss analysis

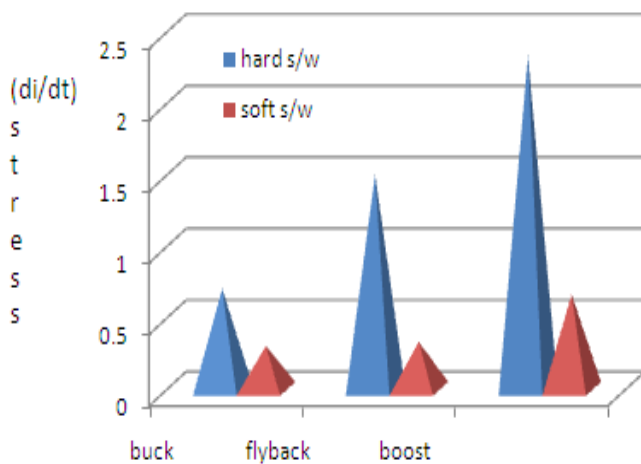
**Stress analysis:**

Fig.24 Graphical view of stress analysis

**VIII CONCLUSION**

This paper emphasizes different PWM DC/DC buck, boost, Flyback converters with Zero Current Transition. The concept of resonance is implemented by using capacitance and inductance (Auxiliary circuit) in all the converters. An suitable converter PWM strategy is designed for the entire control range of frequencies, such that the power switching device IGBT current and voltage waveforms do not overlap, which result in reduced switching losses results in improved converter efficiency. Design of the same presented for a certain switching frequency and simulated by using MATLAB-Simulink. Switching stress and power loss analysis is also carried out for the proposed topologies. Comparison between hard switched and soft switched converters proves that a dc-dc converter switched with ZCT has reduced switching stress and less switching losses which adversely improve the efficiency and reliability entire converter system.

**IX REFERENCES**

- [1] G. Hua, E. X. Yang, Y. Jiang, and F. C. Lee, "Novel zero-current-transition PWM converters," IEEE Trans. Power Electron., vol. 9, no. 6, pp. 601–606, Nov. 1994.
- [2] H. Mao, F. C. Lee, X. Zhou, H. Dai, M. Cosan, and D. Boroyevich, "Improved zero-current transition converters for high power applications," IEEE Trans. Ind. Appl., vol. 33, no. 5, pp. 1220–1232, Sep./Oct. 1997.
- [3] H. S. H. Chung, S. Y. R. Hui, and W. H. Wang, "A zero-current-switching PWM flyback converter with a simple auxiliary switch," IEEE Trans. Power Electron., vol. 14, no. 2, pp. 329–342, Mar. 1999.
- [4] M. Ilic and D. Maksimovic, "Interleaved zero current transition buck converter," in Proc. IEEE Power Electron. Conf., 2005, vol. 2, pp. 1265–1271.
- [5] D. Y. Lee, M. K. Lee, D. S. Hyun, and I. Choy, "New zero-current transition PWM DC/DC converters without current stress," IEEE Trans. Power Electron., vol. 18, no. 1, pp. 95–104, Jan. 2003.
- [6] C. M. Wang, C. H. Su, and C. W. Tao, "Zero-current-transition PWM DC-DC converters using new zero current switching PWM switch cell," Proc. Inst. Electr. Eng.—Electr. Power Appl., vol. 153, no. 4, pp. 503–512, Jul. 2006.
- [7] P. Das and G. Moschopoulos, "A zero-current-transition converter with reduced auxiliary circuit losses," IEEE Trans. Power Electron., vol. 22, no. 4, pp. 1464–1471, Jul. 2007.



[8] E. Adib and H. Farzanehfard, "New zero current transition PWM converters," in Proc. IEEE ICIT Conf., 2006, pp. 2131–2136.

[9] P. Das and G. Moschopoulos, "A comparative study of zero-current transition PWM converters," IEEE Trans. Ind. Electron., vol. 54, no. 3, pp. 1319–1328, Jun. 2007.



M.Prathap Raju , received his B.Tech degree, 2003 from G. Pulla Reddy Engineering College and M.Tech(Power electronics) from JNTUH, Hyderabad, AP, India. He is currently pursuing Ph. D from JNTUH and the paper is carried out

towards the research objective. He is currently working as sr. Assistant professor, Dept of EEI, College of engineering Studies, University of Petroleum and Energy Studies, Dehradun, India.



Dr.A.Jayalaksmi, received her B.Tech degree from NIT Warangal and M. Tech from Osmania University. Awarded Ph.D from JNTUH, Hyderabad, AP, India, in the year 2007. She has quite a good experience in the industry and research. She is currently working as an Associate Professor in the Dept of EEE, JNTU College of Engineering, JNTUH, Hyderabad,

India.